DMD Fast Forward. Published on May 19, 2023 as DOI: 10.1124/dmd.122.001191
This article has not been copyedited and formatted. The final version may differ from this version.

Original Manuscript

The inhibitor preincubation effect is universal to SLC transporter assays and is only partially eliminated in the presence of extracellular protein

Péter Tátrai*, Csilla Temesszentandrási-Ambrus, Tamás Varga, Zsuzsanna Gáborik

PT, CT-A, TV, ZG: SOLVO Biotechnology, Charles River Laboratories Hungary, Budapest, Hungary

*Corresponding author

DMD Fast Forward. Published on May 19, 2023 as DOI: 10.1124/dmd.122.001191
This article has not been copyedited and formatted. The final version may differ from this version.

Running title: The SLC preincubation effect and protein binding

Corresponding author

Péter Tátrai, Ph.D.

Senior Scientist, Research & Development

SOLVO Biotechnology, Charles River Laboratories Hungary

Science Park, Building B, 4-20 Irinyi József Street, H-1117 Budapest, Hungary

Mobile: +36 30 386 0705

Peter.Tatrai@crl.com

Number of text pages: 39

Number of tables: 5

Number of figures: 7

Number of references: 25

Abstract word count: 249

Introduction word count: 766

Discussion word count: 1648

List of abbreviations

ABC, ATP-binding cassette

AMG, methyl-α-D-glucopyranoside

BSA, bovine serum albumin

DMD Fast Forward. Published on May 19, 2023 as DOI: 10.1124/dmd.122.001191
This article has not been copyedited and formatted. The final version may differ from this version.

CCK8, cholecystokinin octapeptide

DDI, drug-drug interaction

E217βG, estradiol 17-β-glucuronide

E3S, estrone 3-sulfate

ER, efflux ratio

FDA, Food and Drug Administration

HBSS, Hanks' Balanced Salt Solution

HEK293, Human Embryonic Kidney 293

KH, Krebs-Henseleit buffer

MDCKII, Madin-Darby Canine Kidney II

MPP+, 1-methyl-4-phenylpyridinium

NMQ, N-methyl-quinidinium

P_{app}, apparent permeability

PTIP, potentiation of transporter inhibition by preincubation

SLC, solute carrier

tPSA, topological polar surface area

VT, vesicular transport

DMD Fast Forward. Published on May 19, 2023 as DOI: 10.1124/dmd.122.001191
This article has not been copyedited and formatted. The final version may differ from this version.

Abstract

Variation in the methodology of *in vitro* transporter inhibition assays causes wide divergence in reported IC_{50}/K_i data. Notably, although potentiation of transporter inhibition by preincubation (PTIP) has been described, current guidelines do not specifically recommend inhibitor preincubation, only encourage sponsors to follow emerging literature. To clarify how generally preincubation should be considered in transporter inhibition studies, and whether PTIP can be solely explained by protein binding of the respective inhibitors, we performed *in vitro* inhibition assays on SLC and ABC transporters scarcely or not covered in prior research, and examined the effect of extracellular protein in preincubation and washout experiments. In SLC assays without extracellular protein, a 30-minute preincubation caused significant >2-fold change of IC_{50} in 21/33 transporter-inhibitor combinations involving 19 evolutionarily disparate transporters. The preincubation effect correlated with inhibitor properties like protein binding and aqueous solubility. In vesicular transport assays of MDR1, BCRP, MRP2, and BSEP, sizable PTIP was observed for only 2/23 combinations, and preincubation was practically inconsequential in BCRP or MDR1 monolayer assays. In SLC assays, PTIP partly persisted in the presence of 5% albumin, indicating that the absence of extracellular protein does not fully explain PTIP. The presence of protein, however, complicated the interpretation of results. Overall, while preincubating without protein may overpredict inhibitory potency, adding protein compromises clarity, and omitting preincubation altogether may miss clinically relevant inhibitors. Therefore, we propose that protein-free preincubation should be considered in all SLC inhibition assays. ABC inhibition seems less commonly affected by preincubation, but conclusions require further investigation.

Significance statement

Drugs may inhibit transporter proteins in the body, which may precipitate drug interactions. *In vitro* transporter inhibition assays help predict such drug interactions. Some inhibitors act more

DMD Fast Forward. Published on May 19, 2023 as DOI: 10.1124/dmd.122.001191
This article has not been copyedited and formatted. The final version may differ from this version.

potently when preincubated with the transporter prior to the assay. Here we argue that this effect is not a mere *in vitro* artefact due to the lack of plasma proteins and should be considered in all uptake inhibition assays to model the worst-case scenario. Preincubation in efflux transporter inhibition assays is likely dispensable.

DMD Fast Forward. Published on May 19, 2023 as DOI: 10.1124/dmd.122.001191
This article has not been copyedited and formatted. The final version may differ from this version.

Introduction

Significant *in vitro* inhibition of a pharmacologically relevant transporter may predict the risk of drug-drug interactions (DDI) and may thus call for further assessment in preclinical animal models (International Transporter Consortium, 2010). Whether *in vitro* inhibition is considered significant depends on the relationship between the unbound concentration of the drug in the relevant body fluid compartment and its experimentally determined inhibition constant (Ki) or half-maximal inhibitory concentration (IC_{50}) (International Transporter Consortium, 2010). *In vitro* measures of inhibitory potency are, however, laden with uncertainty due to wide inter-laboratory variation in assay methodology (McFeely et al., 2020). Experimental conditions for transporter inhibition assays are only broadly delineated in regulatory guidelines. In particular, the finalized FDA guidance for industry (Food and Drug Administration, 2020) contains no clear instruction on the need for preincubation with the test article. Although the 2017 draft version of the guidance (Food and Drug Administration, 2017) recommended a 30-minute preincubation with the putative inhibitor prior to coincubation with the probe substrate, this advice has been removed from the 2020 final version, leaving the decision open to the sponsor's consideration. Similarly, the recently published draft ICH guideline M12 on drug interaction studies (International Council for Harmonisation of Technical Requirements for Pharmaceuticals for Human Use, 2022), while encourages sponsors to follow current literature on the topic, does not explicitly endorse a particular protocol with or without preincubation. Unsurprisingly, the work cited above (McFeely et al., 2020) has identified preincubation as a major source of interlaboratory variability in reported IC_{50} values.

In uptake transporter inhibition assays, it is now generally accepted that preincubation prior to coincubation may increase the apparent inhibitory potency of the test drug. Potentiation of transporter inhibition by preincubation (PTIP) was first reported for the hepatic uptake transporters OATP1B1 and OATP1B3 and a limited set of inhibitors, namely cyclosporin A

DMD Fast Forward. Published on May 19, 2023 as DOI: 10.1124/dmd.122.001191
This article has not been copyedited and formatted. The final version may differ from this version.

(Amundsen et al., 2010; Izumi et al., 2015), saquinavir, and ritonavir (Shitara et al., 2013). These drugs have been proposed to inhibit OATP1Bs *in trans* as well as *in cis*, and incorporation of both inhibition modes into a physiologically based pharmacokinetic model improved alignment with *in vivo* data (Shitara and Sugiyama, 2017). In our previous work we have shown that PTIP, rather than being restricted to OATP1Bs and a handful of drugs, is a prevalent phenomenon across uptake transporters and their inhibitors (Tátrai et al., 2019). Our data also suggested that PTIP was influenced by the physicochemical properties – especially the size and hydrophobicity – of the inhibitor and the duration of coincubation rather than the transporter itself, lending to the notion that PTIP may ultimately be governed by transporter-independent factors like membrane permeability and protein binding.

While our results indicated that PTIP may affect a wider range of uptake transporters than originally thought and hence be of more general interest, many questions remained unresolved. In our initial work, out of theoretical considerations we chose an extended preincubation time of 3 hours, which might be difficult to apply in practice. But how commonly would a shorter preincubation of 30 minutes, as recommended by the 2017 FDA draft guidance (Food and Drug Administration, 2017), still make a meaningful difference in IC_{50}? Also, we originally investigated the FDA-featured panel of transporters (OATP1B1 and 1B3, OAT1 and 3, OCT1 and 2, MATE1 and 2-K) only. Since all of these belong to a relatively close kinship within the SLC superfamily, it remained to be seen whether PTIP is genuinely universal across all SLC transporters, many of which are of emerging clinical interest either as mediators of specific drug interactions or for being promising drug targets. Moreover, if PTIP is not linked to the mechanism of transport, shall we anticipate a preincubation effect in efflux transporter inhibition assays as well?

More pressing were some concerns touching on the very essence of PTIP. *In vitro* inhibition assays are typically performed in protein-free buffers, even when the test compound is known to be highly protein-bound *in vivo*. During an extended preincubation time, such compounds may

DMD Fast Forward. Published on May 19, 2023 as DOI: 10.1124/dmd.122.001191
This article has not been copyedited and formatted. The final version may differ from this version.

accumulate disproportionately within the cells due to intracellular protein binding (Izumi et al., 2022). Could PTIP as a whole be an *in vitro* artefact caused by the lack of extracellular protein and consequent intracellular accumulation of the inhibitor during preincubation? How much, if any, of the preincubation effect remains if the *in vivo* extracellular protein concentration is being mimicked?

In pursuit of answers, we have assessed PTIP with selected inhibitors using a shortened, 30-minute preincubation, extended the study of PTIP to additional SLC transporters as well as representative members of the ABC transporter family, and investigated the effect of extracellular protein on PTIP in both preincubation and washout experiments.

Materials and Methods

Chemicals

Dapagliflozin, eltrombopag, rosuvastatin, and tenofovir were purchased from Carbosynth; talinolol was from Cayman Chemical; sulfated cholecystokinin octapeptide (CCK8) was from Tocris; riboflavin 5'-phosphate (flavin mononucleotide) was from MedChemExpress; N-methyl-quinidinium (NMQ) iodide was from Biological Research Center (Szeged, Hungary); nanvuranlat (JPH203) was from SelleckChem; all other non-radiolabeled chemicals were from Sigma/Merck. Radiochemicals were obtained from PerkinElmer (^{3}H-CCK8, ^{3}H-E217βG, ^{3}H-L-serine, ^{3}H-L-leucine, ^{3}H-MPP+, ^{3}H-prazosin, ^{3}H-taurocholic acid), Moravek (^{14}C-metformin, ^{14}C-uric acid, ^{3}H-cGMP, ^{3}H-riboflavin, ^{3}H-tenofovir, ^{3}H-uridine), American Radiolabeled Chemicals (^{14}C-AMG, ^{3}H-digoxin, ^{3}H-sumatriptan), and the Szeged Biological Research Center (^{3}H-E3S, ^{3}H-NMQ).

Cell lines

DMD Fast Forward. Published on May 19, 2023 as DOI: 10.1124/dmd.122.001191
This article has not been copyedited and formatted. The final version may differ from this version.

MDCKII-MDR1 cells were purchased from Creative Cell Ltd. (Budapest, Hungary). All other cell lines stably overexpressing SLC and ABC transporters were created in house using standard lentiviral gene delivery technique. Cell lines used for cellular uptake inhibition experiments and those used for membrane vesicle preparation were generated from HEK293 (Life Technologies), except for those expressing CNT1, CNT2, CNT3, ENT1, ENT2, MCT8, MCT10, and URAT1, which were generated from MDCKII (ECACC). All cell lines were derived from single-cell colonies that were amplified and tested for optimal transporter function and growth properties. Cell cultures were maintained in Dulbecco's Modified Eagle's Medium (with 4500 mg/L glucose, GlutaMAX™, and sodium pyruvate), 10% v/v fetal bovine serum, and penicillin/streptomycin (all from Thermo Fisher). For cellular uptake inhibition experiments, cells overexpressing SLC transporters, along with appropriate mock-transduced controls, were seeded into 96-well tissue culture plates at a density of 100,000 cells / well 20-24 hours prior to the experiment. Plates pretreated with poly-D-lysine were used for HEK293-based cell lines. No control cells were seeded in the LAT1 assay; instead, control wells were also seeded with HEK293-LAT1 but 10 μM nanvuranlat (JPH203) was added to the assay buffer during both preincubation and the assay. For vesicular transport experiments, purified membrane vesicles were prepared from HEK293 cells overexpressing MDR1 or BCRP as described previously (Sarkadi et al., 1992). The protein content of membrane suspensions was determined by the bicinchoninic acid (BCA) method (Sigma-Aldrich), total protein concentration was set to 5 mg/mL, and suspensions were stored at -80°C until use. For monolayer inhibition experiments, MDCKII-MDR1, MDCKII-BCRP, and MDCKII control cells were seeded into 96-well Millicell cell culture insert plates (Millipore) at a density of 25,000 cells / well and allowed to form a confluent, tight monolayer for 4 days prior to the experiment.

Cellular uptake inhibition assays

DMD Fast Forward. Published on May 19, 2023 as DOI: 10.1124/dmd.122.001191
This article has not been copyedited and formatted. The final version may differ from this version.

Following aspiration of the cell culture medium, cells were rinsed twice with pre-warmed assay buffer, which was Krebs-Henseleit buffer (KH: 110 mM NaCl, 24.0 mM $NaHCO_3$, 4.80 mM KCl, 1.00 mM K_2HPO_4, 1.20 mM $MgSO_4$, 13.0 mM HEPES, 5.00 mM glucose, 1.53 mM $CaCl_2$), pH 8.0, for MATE1, MATE2-K, ASCT1, and ASCT2; KH, pH 7.4, for CNT1, CNT2, CNT3, ENT1, ENT2, and RFVT3; sodium-free KH (choline chloride and choline bicarbonate replacing NaCl and $NaHCO_3$, respectively), pH 7.4, for LAT1; sodium-free MCT uptake buffer (124.9 mM NaCl, 5.00 mM KCl, 0.98 mM $CaCl_2$, 1.20 mM $MgCl_2$, 10.0 mM HEPES, 5.09 mM glucose), pH 7.4, for MCT8 and MCT10; and Hanks' Balanced Salt Solution (HBSS: 138 mM NaCl, 4.17 mM $NaHCO_3$, 0.336 mM Na_2HPO_4, 5.33 mM KCl, 0.441 mM KH_2PO_4, 0.406 mM $MgSO_4$, 0.493 mM $MgCl_2$, 1.26 mM $CaCl_2$, 5.56 mM glucose), pH 7.4, for all other transporters. In SGLT assays, glucose in the buffer was isosmotically replaced by NaCl; glucose-free KH was used for SGLT1 and glucose-free HBSS was used for SGLT2. After the washes cells were preincubated either with the inhibitor or its solvent diluted in assay buffer for the durations specified. Probe substrates, inhibitors and their concentrations used during the uptake step are listed in Table 1 or the corresponding text. In the ASCT1 assay, the activity of endogenous ASCT2 was blocked by adding 20 mM L-glutamine to the reaction mixture. Preincubation and uptake were performed at 25°C for ASCT1 and ASCT2, and at 37°C for all others. Bovine serum albumin (BSA; protease-, fatty acid- and globulin-free, Sigma-Aldrich) was added during the preincubation step, the uptake step, neither, or both, as indicated in the text. In all assays except for MCT8 and MCT10, uptake was terminated by aspirating the reaction mixture and washing the wells twice with assay buffer pre-chilled on ice. Cells were then either lysed directly with liquid scintillation cocktail (Ultima Gold, PerkinElmer) or with 0.1N NaOH and the lysate was mixed with scintillation cocktail. Cellular accumulation of the radiolabeled substrate was read in a MicroBeta^2 (PerkinElmer) microplate counter. In the MCT8 and MCT10 assays, aspiration of the reaction mixture was followed by two washes with ice-cold assay buffer containing additional 0.1% w/v BSA and two washes with ice-cold purified water. Cells were then lysed with 0.68 M

DMD Fast Forward. Published on May 19, 2023 as DOI: 10.1124/dmd.122.001191
This article has not been copyedited and formatted. The final version may differ from this version.

ammonium persulfate at 90°C for 60 minutes, and the accumulation of triiodothyronine was quantified by means of the Sandell-Kolthoff reaction. Briefly, 5 volumes of sodium arsenite solution (25 mM $NaAsO_2$, 0.5 M H_2SO_4, 0.2 M NaCl) and 5 volumes of acidic ammonium cerium(IV) sulfate reagent (25 mM $(NH_4)_4Ce(SO_4)_4$ dissolved in 0.5 M H_2SO_4) were added to 1 volume of the cell lysates, and optical density at 415 nm (OD_{415}) was followed up for 21 cycles, 1 minute each, in a FLUOstar Omega plate reader (BMG Labtech). The amount of iodine in each sample was calculated from the slope of the ΔOD_{415} curve.

Vesicular transport inhibition assays

Transporter-specific reagents and reaction conditions of vesicular transport assays are detailed in **Supplementary Table 1.** Briefly, membrane vesicles from HEK293 cells overexpressing MDR1, BCRP, BSEP, or MRP2 were thawed, diluted in transport buffer, dispensed into a flat-bottom 96-well tissue culture plate, and preincubated with the inhibitor or its solvent at assay temperature. After 30 minutes, a reaction mixture containing the probe substrate, 4 mM ATP, and the inhibitor was added to initiate ATP-dependent transport. In control wells, ATP was substituted for by AMP. The reaction was stopped by the addition of wash buffer pre-chilled on ice. The contents of each well were transferred to a 96-well filter plate (MultiScreen®HTS-FB, Millipore), and the membrane vesicles were washed 5 times with the same buffer using a rapid filtration device. For the detection of radiolabeled probe substrates, liquid scintillation cocktail (Ultima Gold, PerkinElmer) was added to the vesicles, and accumulated radioactivity was quantified in a MicroBeta^2 (PerkinElmer) microplate counter. For the detection of coproporphyrin I, vesicles were lysed with 0.1 M NaOH, and fluorescence at Ex: 355 nm / Em: 620 nm was measured in a FLUOstar Omega plate reader.

DMD Fast Forward. Published on May 19, 2023 as DOI: 10.1124/dmd.122.001191
This article has not been copyedited and formatted. The final version may differ from this version.

Monolayer inhibition assays

Cell culture inserts were transferred to the appropriate 96-well receiver tray, and following aspiration of the culture medium cells were preincubated for 30 minutes (BCRP) or 60 minutes (MDR1) at 37°C either with 0.1% DMSO (inhibitor vehicle) or the dilutions of the inhibitor prepared in HBSS. The inhibitor / vehicle was added to both the apical and basolateral compartments. The preincubation solution was aspirated and replaced by reaction mixture containing inhibitor dilutions and the probe substrate in HBSS. Unlike the inhibitor that was added to both compartments, the probe substrate was either added apically to assess apical-to-basolateral transport, or basolaterally to assess basolateral-to-apical transport. The initial concentration of the probe substrate, digoxin or prazosin, in the donor compartment was 5 μM or 1 μM for MDR1 and BCRP, respectively, and in each case included 0.0188 μCi/mL radiotracer. Both the donor and receiver compartments were sampled after 60 minutes (BCRP) or 120 minutes (MDR1) of incubation at 37°C. Samples were mixed with scintillation cocktail, and the radiotracer transported across the monolayer was quantified in a MicroBeta^2 (PerkinElmer) microplate counter.

Calculations

All experimental conditions were run in triplicate wells on 96-well plates. In uptake inhibition assays, each condition was tested in parallel on transporter-overexpressing and mock-transduced control cells (or, in the case of LAT1, in the absence and presence of the LAT1 blocker nanvuranlat), and transporter-specific uptake was calculated by subtracting the mean uptake of control cells (or LAT1-blocked cells) from the mean uptake of transporter-overexpressing cells. Relative transporter-specific transport was calculated as specific transport at each inhibitor concentration over specific transport in the absence of the inhibitor, and IC_{50}

DMD Fast Forward. Published on May 19, 2023 as DOI: 10.1124/dmd.122.001191
This article has not been copyedited and formatted. The final version may differ from this version.

curves were fitted to these values by nonlinear regression in GraphPad Prism 9 (GraphPad Software). In vesicular transport inhibition experiments, each condition was measured in the presence of either ATP or AMP, and mean values measured with AMP were subtracted from mean values measured with ATP to calculate transporter-specific transport. Relative transporter-specific transport was calculated and curves were fitted analogously to the uptake experiments. In monolayer inhibition experiments, normalized net efflux ratio at each inhibitor concentration was calculated in multiple steps. First, apparent permeability (P_{app}) of the probe substrate in both directions ($P_{app,\ A\text{-}B}$: apical-to-basolateral; $P_{app,\ B\text{-}A}$: basolateral to apical) was determined as $P_{app} = (\Delta Q/\ \Delta t)\times(1/(A \times C_0))$, where ΔQ is the amount of substrate translocated to the receiver compartment by the end of incubation, Δt is the duration of incubation, A is the surface area of the insert membrane, and C_0 is the initial concentration of the substrate in the donor compartment. Second, efflux ratio (ER) was calculated as $P_{app,\ B\text{-}A}$ / $P_{app,\ A\text{-}B}$. For MDR1, ER was determined in both MDCKII-MDR1 and MDCKII control cells, and net ER was calculated by subtracting $ER_{control}$ from ER_{MDR1} to account for the background activity of endogenous canine MDR1. Finally, (net) ER values were forced between 0 and 1 by calculating normalized (net) ER at each inhibitor concentration as $([net]ER_{inhibitor}\text{-}1)/([net]ER_{vehicle}\text{-}1)$, where $(net)ER_{inhibitor}$ is the (net) ER determined at any given concentration of the inhibitor and $(net)ER_{vehicle}$ is the (net) ER in the presence of the inhibitor vehicle only. IC_{50} curves were fitted to normalized (net) ER values by nonlinear regression in GraphPad Prism 9 using the constraints Bottom=0 and Top=1.

Statistics

IC_{50} values measured with and without preincubation were compared by Student's t-test in Microsoft Excel. All other statistics were performed in GraphPad Prism 9. Spearman's and Pearson's correlation coefficients were calculated between PTIP and each molecular descriptor.

DMD Fast Forward. Published on May 19, 2023 as DOI: 10.1124/dmd.122.001191
This article has not been copyedited and formatted. The final version may differ from this version.

Contingency tables of PTIP predictors were analyzed by Fisher's exact test. In each case, $p<0.05$ was considered significant.

Results

The effect of a 30-minute preincubation on IC_{50} in SLC transporter inhibition assays

Selected PTIP experiments previously carried out with a 3-hour preincubation were repeated with the duration of preincubation reduced to 30 minutes, and additional transporter/inhibitor pairs were also investigated with a 30-minute preincubation step. The 30-minute PTIP, or $PTIP_{30min}$, was expressed as the fold decrease in IC_{50} upon a 30-minute preincubation with inhibitor dilutions as compared to preincubation with the inhibitor vehicle (**Table 1**). While preincubation with L-cysteine, probenecid, rifamycin SV, rifampicin, adenosine, dipyridamole, phloridzin, or deoxycytidine did not significantly change the IC_{50} for any of the transporters tested (highest $PTIP_{30min} < 2.00$ and/or difference not significant), the other 15 inhibitors tested had the potential to cause significant $PTIP_{30min} \geq 2.00$ in at least one transporter assay. When comparing current and prior results, the effect of a 30-min preincubation on IC_{50} was not consistently smaller than the effect of a 3-hour preincubation ($PTIP_{30min} < PTIP_{3h}$ in 5/11 cases) (**Supplementary Table 2**).

The relation of PTIP to SLC phylogeny

Phylogenetic mapping of all human transporters for which $PTIP_{30min} \geq 2.00$ was observed reveals no exclusive association of PTIP with any single evolutionary branch of the SLC phylogenetic tree (**Figure 1**). Of the 6 major phylogenetic branches of SLC transporters, G1-G6 (Zhang et al., 2019), we studied transporters falling into subdivisions G3-G6, and $PTIP_{30min} \geq 2.0$

DMD Fast Forward. Published on May 19, 2023 as DOI: 10.1124/dmd.122.001191
This article has not been copyedited and formatted. The final version may differ from this version.

was confirmed on all 4 branches investigated; namely, in G3 (OATs, OCTs, and URAT1, all in the SLC22 family), G4 (OATP1Bs in the SLCO family, MATEs in the SLC47 family, RFVT3 in the SLC52 family, and MCTs in the SLC16 family), G5 (ENT1 in the SLC29 family), and G6 (ASBT and NTCP in the SLC10 family, LAT1 in the SLC7 family, and SGLT2 in the SLC5 family). Transporters on branches G1 and G2 were not included in this study.

The relation of PTIP to the physicochemical properties of the inhibitor

To identify potential links between PTIP and the physicochemical properties of inhibitors, correlation of highest observed $PTIP_{30min}$ with molecular class (acid/base vs. neutral/zwitterionic), molecular weight, calculated LogD pH7.4 (CX LogD), calculated LogP (CX LogP), topological polar surface area (tPSA), calculated solubility (CLogS), and predicted plasma protein binding (PPB_p) was analyzed (**Table 2**; a color-enhanced version of this table is provided as **Supplementary Figure 1**). While $PTIP_{30min}$ showed no significant correlation with MW or tPSA, $PTIP_{30min}$ was modestly correlated with CX LogD and CX LogP, and markedly correlated with PPB_p as well as inversely with CLogS (**Figure 2, A-F**). $PTIP_{30min}$ was also found to be inversely correlated with a derived parameter, tPSA/MW, which can be interpreted as the polar surface area adjusted for molecule size (**Figure 2, G**). tPSA/MW was a reliable predictor of PTIP, since all 12 inhibitors with tPSA/MW ratio ≤ 0.25, as opposed to only 3 out of 11 inhibitors with tPSA/MW ratio > 0.25, displayed highest $PTIP_{30min}$ ≥ 2.00 (Fisher's exact test, sensitivity=1.00, specificity=0.80, P=0.0003). Also, acids and bases were more likely to display PTIP, as 9 out of 10 (90%) acids/bases but only 6 out of 13 (46%) neutrals/zwitterions had a highest $PTIP_{30min}$ ≥ 2.00; however, this tendency was not significant (Fisher's exact test, P=0.0743).

DMD Fast Forward. Published on May 19, 2023 as DOI: 10.1124/dmd.122.001191
This article has not been copyedited and formatted. The final version may differ from this version.

The effect of preincubation in vesicular transport (VT) inhibition assays of MDR1, BCRP, BSEP, and MRP2

To assess whether preincubation enhances inhibition of pharmacologically relevant ABC efflux transporters in the VT assay, inhibitors of MDR1 (ABCB1), BCRP (ABCG2), BSEP (ABCB11), and MRP2 (ABCC2) were first pre-screened at a high and a low concentration (selected to be above and below the previously established IC_{50}, respectively) with and without preincubation (**Supplementary Figure 2**). Of the 20 inhibitors tested, 9 exhibited PTIP greater than 20% at either concentration when a 30-minute preincubation was applied. These inhibitors were followed up in IC_{50} experiments with and without preincubation (**Table 3** and **Figure 3**), which were conducted twice if a PTIP > 2-fold was seen in the first instance. Mean PTIP marginally greater than 2-fold was observed for two MDR1 inhibitors, valspodar and zosuquidar, but the difference in IC_{50} was significant (P=0.028) for valspodar only.

The effect of preincubation on monolayer inhibition assays of BCRP and MDR1

The effect of preincubation on the inhibition of the same predominant efflux transporters, BCRP and MDR1, was investigated in the transcellular permeability (a.k.a. monolayer) assay using standard inhibitors for each transporter, all of which were tested in the VT assay as well (Ko-143, omeprazole, and eltrombopag for BCRP; valspodar, zosuquidar, quinidine, and verapamil for MDR1) (**Table 4** and **Supplementary Figure 3**). The duration of preincubation / coincubation was 30 min / 60 min for BCRP and 60 min / 120 min for MDR1. No significant decrease in IC_{50} upon preincubation with the inhibitor was noted in any of the assays.

The modifying effect of bovine serum albumin on PTIP in uptake inhibition assays

DMD Fast Forward. Published on May 19, 2023 as DOI: 10.1124/dmd.122.001191
This article has not been copyedited and formatted. The final version may differ from this version.

We returned to uptake transporters to investigate whether the addition of bovine serum albumin (BSA) to the assay buffer eliminates the preincubation effect we observe when no extracellular protein is present. For proof-of-concept experiments we selected two prototypical PTIP(+) inhibitors, the OAPT1B1/OATP1B3 inhibitor venetoclax and the OCT1/OCT2 inhibitor ledipasvir.

Preincubation was performed for 3 hours with or without the inhibitor in the absence of protein or with graded concentrations (1%, 2%, 4%, and 5% w/v) of BSA in the buffer. The subsequent coincubation step was either run without protein, to avoid potential interference of the probe substrate with BSA (**Figure 4**), or with protein added at the same concentration as during preincubation (**Figure 5**). In the first setting (no protein during coincubation), 2% to 5% w/v BSA in the preincubation buffer mostly offset the preincubation effect of 0.3 μM venetoclax; however, when a higher venetoclax concentration of 3.0 μM was applied, preincubation even in the presence of 5% w/v BSA resulted in 2-fold excess inhibition. Consistently, 4-5% w/v BSA reduced the preincubation effect of 0.1 μM ledipasvir from 5-fold to 2.5-fold excess inhibition, but no amount of BSA up to 5% w/v was able to reverse the 10-fold excess inhibition caused by preincubation with 1.0 μM ledipasvir.

In the second setting (protein during both preincubation and coincubation), a sharp decline in signal intensity with increasing concentrations of BSA was readily apparent, especially with E217βDG as a substrate. This effect was likely explained by the binding of the substrate (E217βDG in particular) to BSA, which also occurred without any inhibition (**Figure 6**). The attenuating effect of BSA on PTIP was more pronounced but otherwise similar to that seen in the first setting: BSA opposed PTIP in a concentration-dependent manner but failed to fully reverse excess inhibition caused by preincubation. With 5% w/v BSA present during both preincubation and coincubation, preincubation-dependent excess inhibition was only ~10% and ~30% for venetoclax at 0.3 μM and 3.0 μM, respectively, but remained as high as ~50% (2-fold) and ~75% (4-fold) for ledipasvir at 0.1 μM and 1.0 μM, respectively.

DMD Fast Forward. Published on May 19, 2023 as DOI: 10.1124/dmd.122.001191
This article has not been copyedited and formatted. The final version may differ from this version.

Next, we investigated how the addition of 5% w/v BSA influences the IC_{50} shift caused by a 30-minute preincubation (**Table 5**). Preincubation with known PTIP(+) inhibitors was performed with the inhibitor or its solvent in the presence or absence of 5% w/v BSA. The uptake assay was invariably performed without BSA, but in addition to standard coincubation (concomitant application of the substrate and the inhibitor) we also tested a washout condition where the substrate alone was applied while the inhibitor was no longer present during the uptake phase.

Except for ledipasvir where the 30-minute preincubation was insufficient to elicit substantial inhibition, all other inhibitors caused PTIP ≥ 2.5 when preincubation was done without BSA. When 5% w/v BSA was added during preincubation, PTIP still remained ≥ 2.5 for venetoclax, cyclosporin A, and irinotecan, but not for daclatasvir and isavuconazole. Withdrawing the inhibitor during the uptake phase blunted or even canceled the effect of preincubation, which may indicate a need for the presence of the inhibitor both *in cis* and *in trans* for efficient inhibition. Strikingly, however, preincubation with venetoclax (both with and without BSA) and isavuconazole (without BSA) was persistent enough to cause stronger inhibition compared to coincubation even when the inhibitor was removed during substrate uptake.

The effect of BSA on the persistence of inhibition during washout

Lastly, we investigated the persistence of the preincubation effect after different periods (0, 15, 30, 60, and 90 minutes) of washout, with no protein vs. 1% w/v BSA or 5% w/v BSA in the medium during the washout phase (**Figure 7**). Preincubation was done for 90 minutes in protein-free medium. When no BSA was present during the washout, uptake inhibition caused by preincubation with venetoclax (OATP1B1) or ledipasvir (OCT1) remained largely invariant up to 90 minutes. For ledipasvir, the presence of 1% w/v BSA did not markedly alter this behavior, while with 5% w/v BSA during washout a slow decline in inhibition (from 40% / 76% [1 μM / 10

μM] inhibition directly after pre-incubation to 19% / 63% inhibition after 60 minutes of washout) was observed. By contrast, the inhibitory effect of venetoclax declined rapidly when either 1% or 5% w/v BSA was present during washout.

Discussion

We have shown previously that a 3-hour inhibitor preincubation in selected uptake transporter inhibition assays may alter the outcome of DDI risk assessment by substantially decreasing IC_{50} (Tátrai et al., 2019). Here we demonstrate that a shortened 30-minute preincubation, as recommended by the 2017 draft version of the FDA guidance (Food and Drug Administration, 2017), is often sufficient to cause a PTIP > 2.0. Although for some compounds the preincubation effect may continue to increase after 30 minutes and may require over 3 hours to plateau (Tátrai et al., 2019), when comparing our prior and current data we did not note a general tendency of PTIP becoming smaller upon reducing the preincubation time from 3 hours to 30 minutes, and marked PTIP with tyrosine kinase inhibitors and MATE1 was observed by others after only 15 minutes of preincubation (Uddin et al., 2021). Therefore, a 30-minute duration may optimally combine sensitivity with practical feasibility.

While our prior results were restricted to a close kinship within the SLC superfamily, here we demonstrate that transporters affected by PTIP are ubiquitous across SLC phylogeny and display great structural and functional diversity. For example, OATPs have 12 predicted transmembrane domains with intracellular termini and perform sodium-independent electroneutral exchange (Roth et al., 2012), whereas SGLT2 has 14 predicted transmembrane domains with extracellular termini and operates by electrogenic sodium cotransport (Wright et al., 2011). Therefore, PTIP is unlikely to depend on any specific structural or mechanistic feature of an individual SLC transporter or even subgroup. Although no PTIP > 2.0 was

DMD Fast Forward. Published on May 19, 2023 as DOI: 10.1124/dmd.122.001191
This article has not been copyedited and formatted. The final version may differ from this version.

confirmed for 9 out of 30 SLC transporters investigated, we argue that the lack of observed PTIP is not explained by the structure or mechanism of a transporter but by a lack of inhibitors that qualify for PTIP either because of their physicochemical properties or due to behaving as substrates.

If, however, PTIP is dictated by the inhibitor and not the transporter, it might as well occur in conjunction with ABC transporters. *Trans*-inhibition has been documented not only for multiple SLC transporters including OATPs (Shitara and Sugiyama, 2017), OATs (Duan and You, 2009), and OCTs (Zhang et al., 2000), but also for MDR1 (Jutabha et al., 2010) and BSEP (ABCB11) (Vallejo et al., 2006), albeit the latter studies were conducted on *Xenopus* oocytes rather than membrane vesicles.

In our VT experiments with MDR1, BCRP, BSEP, and MRP2, 9 out of 20 inhibitors displayed >20% enhancement of inhibition upon a 30-minute preincubation, typically at high (above IC_{50}) concentrations. Such enhancement was predominantly seen in the 1-minute assays of MDR1 and BCRP. In these short-duration assays, extended equilibration time provided by preincubation occasionally resulted in a PTIP-like effect which, however, with the single exception of valspodar, did not translate into significant >2-fold decreases of IC_{50}. Also, no significant preincubation effect was confirmed in monolayer inhibition assays of MDR1 and BCRP. Of note, our routine VT assays contain a 15-minute preincubation step that facilitates inhibitor equilibration. No-preincubation vs. 30-minute preincubation VT assay pairs were conducted for the purpose of this study to match the experimental design of uptake inhibition assays.

While the rarity of significant PTIP in the vesicular assay may be explained, e.g., by rapid equilibration of the inhibitor into the small, protein-free inner matrix of membrane vesicles, the monolayer assay is a cellular model system where the inhibitor needs to permeate into the cell to act *in cis* with the substrate; thus, delayed equilibration of the inhibitor with the intracellular

DMD Fast Forward. Published on May 19, 2023 as DOI: 10.1124/dmd.122.001191
This article has not been copyedited and formatted. The final version may differ from this version.

compartment could potentially cause PTIP. Nonetheless, a marked and consistent preincubation effect would be intriguing, as monolayer assays are very long compared to a typical uptake assay (60-120 min vs. 1-15 min), and extended coincubation is expected to dampen the additional effect of preincubation.

Although transmembrane permeation of the inhibitor is a common determinant in both cellular and vesicular assays and may contribute to PTIP, cellular assays have a unique feature: here, the extracellular side of the membrane commonly faces a protein-free buffer, while the other side faces the cytoplasm, a dense proteinaceous matrix. This setup contrasts with the vesicular assay where both the medium and the vesicular lumen are typically protein-free. For highly protein-bound inhibitors, the cellular interior may act like a sponge that absorbs massive amounts of the inhibitor until the unbound fractions equilibrate across the membrane. This was demonstrated in our previous paper (Tátrai et al., 2019) as well as in a recent study where the intracellular accumulation of cyclosporin A reached a plateau after approx. 60 minutes at a cell-to-buffer concentration ratio of 3930 (Izumi et al., 2022). The time to reach this steady state is essentially governed by two factors, both largely (albeit not solely) dependent on the physicochemical properties of the inhibitor: permeability and protein binding. The major question is the relative contribution of these two factors to PTIP. If protein binding alone accounts for the whole phenomenon, PTIP may be no more than an *in vitro* artefact and preincubation is bound to cause overprediction of inhibitory potency. If, however, PTIP at least partially persists after correcting for the protein bias, preincubation may be physiologically relevant and improve *in vitro* to *in vivo* extrapolation, as suggested recurringly by the Sugiyama group (Shitara and Sugiyama, 2017; Izumi et al., 2022). In the latter case, preincubation would clearly be beneficial for prediction by narrowing the gap between short *in vitro* assay durations and prolonged *in vivo* drug exposure.

DMD Fast Forward. Published on May 19, 2023 as DOI: 10.1124/dmd.122.001191
This article has not been copyedited and formatted. The final version may differ from this version.

In our small dataset of 23 inhibitors, PTIP correlated with lipophilicity and low solubility as well as with predicted protein binding, all of which are cross-related. Therefore, protein binding was confirmed as a likely contributor to the preincubation effect. In spite of that, PTIP was only partially quenched by the addition of extracellular protein. BSA added to the preincubation buffer reversed PTIP of 0.3 μM venetoclax in a concentration-dependent manner, but 3.0 μM venetoclax still caused a 2-fold excess inhibition upon preincubation even in the presence of 5% BSA. Mean peak and trough total plasma concentrations of venetoclax in leukemia patients were established as 2966 ng/mL (3.41 μM) and 1018 ng/mL (1.17 μM), respectively (Yang et al., 2022); thus, 3.0 μM is a clinically relevant concentration. The preincubation effect of ledipasvir was even more resistant to BSA, as it was largely or completely maintained at 0.1 μM / 1.0 μM drug concentrations, respectively, even with 5% added BSA. Again, these concentrations neatly overlap with the therapeutic range as the C_{max} of ledipasvir was measured to be 348-371 ng/mL (0.39-0.42 μM) (German et al., 2016). Hence, the preincubation effect of these drugs, applied in clinically realistic concentrations, partially or fully withstood the addition of 5% BSA during preincubation.

In the absence of extracellular protein, inhibition caused by a 90-minute protein-free preincubation with venetoclax and ledipasvir was remarkably durable: the same extent of inhibition was measured after 0 and 90 minutes of washout. Such persistent effect was described for cyclosporin A as a preincubation-sensitive inhibitor of OATP1B1 (Shitara and Sugiyama, 2017) and OCT1 (Panfen et al., 2019). For venetoclax, addition of BSA during washout gradually reversed this suppression. Notably, however, for ledipasvir no reversal was caused by 1% BSA and only minor reversal was caused by 5% BSA. This suggests that the binding of ledipasvir to cellular proteins, or to the transporter itself, was stable enough to sustain the *trans*-inhibitory effect even when an extracellular protein sink was available.

DMD Fast Forward. Published on May 19, 2023 as DOI: 10.1124/dmd.122.001191
This article has not been copyedited and formatted. The final version may differ from this version.

Looking for accurate drug interaction predictions, the ultimate question is whether and how to include preincubation in our *in vitro* transporter inhibition experiments. Will preincubation help avoid false negative predictions or only aggravate the burden of false positives? And, if we decide to preincubate, shall we do it with or without protein in the buffer? Based on prior knowledge and the data presented herein we propose some aspects for consideration.

0) Preincubation was practically inconsequential in vesicular transport and monolayer inhibition assays of selected efflux transporters. Therefore, based on available evidence we don't see sufficient justification for generally recommending preincubation in these assays. Meanwhile, preincubation should clearly be considered for all uptake inhibition assays since PTIP seems indifferent to the actual SLC transporter investigated. 1) By omitting preincubation we may miss inhibitors that require prolonged equilibration to exert any effect. Venetoclax or ledipasvir are strong inhibitors at clinically relevant concentrations, but only if allowed sufficient time to act. Thus, omission of preincubation may lead to false negative predictions. 2) Massive intracellular accumulation of a highly protein-bound inhibitor may enhance its *trans*-inhibitory effect; therefore, by preincubating without extracellular protein we may, in theory, overpredict inhibition and produce false positives. However, in an assay calibration study with clinically proven perpetrators and non-perpetrators of OATP1B1/1B3-mediated DDI, a 30-minute protein-free preincubation did not cause overprediction of the clinical effect (Sane et al., 2020). 3) If opting to add protein to the buffer we may choose to use it throughout the assay, i.e., during both preincubation and coincubation, or only during preincubation. Protein in the coincubation mixture may sequester the substrate as well and may thus cause substantial signal loss, which can be normalized for but may still undermine the solidity of the assay. On the other hand, adding protein during preincubation only leads to ambiguity, as it is unclear whether unbound inhibitor concentrations (as present during preincubation) or total nominal concentrations (as present during coincubation) should be reported. In other words, while the addition of protein to

the assay buffer may prevent the buildup of artefactually high cellular concentrations of the inhibitor, it raises practical and interpretation issues of its own.

In our view, performing all SLC inhibition assays with a 30-minute preincubation in the absence of extracellular protein provides results that are straightforward to interpret, and may help to minimize the chance of false negative predictions without unacceptably increasing the risk of false positives. Validation of this approach against clinical data has been done for OATP1B1/1B3 (Sane et al., 2020) and is underway for other clinically relevant SLC transporters.

Authorship Contributions

Participated in research design: Tátrai, Temesszentandrási-Ambrus, and Gáborik

Conducted experiments: Tátrai, Temesszentandrási-Ambrus, and Varga

Performed data analysis: Tátrai and Temesszentandrási-Ambrus

Wrote or contributed to the writing of the manuscript: Tátrai and Gáborik

References

Amundsen R, Christensen H, Zabihyan B, Asberg A (2010) Cyclosporine A, but not tacrolimus, shows relevant inhibition of organic anion-transporting protein 1B1-mediated transport of atorvastatin. Drug Metab Dispos. 38: 1499-1504.

Berton P, Mishra MK, Choudhary H, Myerson AS, Rogers RD (2019) Solubility Studies of Cyclosporine Using Ionic Liquids. ACS Omega. 4: 7938-7943.

Duan P, You G (2009) Novobiocin is a potent inhibitor for human organic anion transporters. Drug Metab Dispos. 37: 1203-1210.

Food and Drug Administration (2017) In Vitro Metabolism- and Transporter- Mediated Drug-Drug Interaction Studies Guidance for Industry. Draft Guidance. Available online: https://downloads.regulations.gov/FDA-2017-D-5961-0003/attachment_1.pdf

Food and Drug Administration (2020) In Vitro Drug Interaction Studies — Cytochrome P450 Enzyme- and Transporter-Mediated Drug Interactions Guidance for Industry. Final Guidance Document. Available online: https://www.fda.gov/media/134582/download

German P, Mathias A, Brainard D, Kearney BP (2016) Clinical Pharmacokinetics and Pharmacodynamics of Ledipasvir/Sofosbuvir, a Fixed-Dose Combination Tablet for the Treatment of Hepatitis C. Clin Pharmacokinet. 55: 1337-1351.

International Council for Harmonisation of Technical Requirements for Pharmaceuticals for Human Use (2022) ICH Harmonised Guideline: Drug Interaction Studies M12. Draft. Available online: https://www.ema.europa.eu/documents/scientific-guideline/draft-ich-guideline-m12-drug-interaction-studies-step-2b_en.pdf

International Transporter Consortium, Giacomini KM, Huang SM, Tweedie DJ, Benet LZ, Brouwer KL, Chu X, Dahlin A, Evers R, Fischer V, Hillgren KM, Hoffmaster KA, Ishikawa T, Keppler D, Kim RB, Lee CA, Niemi M, Polli JW, Sugiyama Y, Swaan PW, Ware JA, Wright SH, Yee SW, Zamek-Gliszczynski MJ, Zhang L (2010) Membrane transporters in drug development. Nat Rev Drug Discov. 9: 215-236.

Izumi S, Nozaki Y, Lee W, Sugiyama Y (2022) Experimental and Modeling Evidence Supporting the Trans-Inhibition Mechanism for Preincubation Time-Dependent, Long-Lasting Inhibition of Organic Anion Transporting Polypeptide 1B1 by Cyclosporine A. Drug Metab Dispos. 50: 541-551.

Izumi S, Nozaki Y, Maeda K, Komori T, Takenaka O, Kusuhara H, Sugiyama Y (2015) Investigation of the impact of substrate selection on in vitro organic anion transporting polypeptide 1B1 inhibition profiles for the prediction of drug-drug interactions. Drug Metab Dispos. 43: 235-247.

Jutabha P, Wempe MF, Anzai N, Otomo J, Kadota T, Endou H (2010) Xenopus laevis oocytes expressing human P-glycoprotein: probing trans- and cis-inhibitory effects on [3H]vinblastine and [3H]digoxin efflux. Pharmacol Res. 61: 76-84.

McFeely SJ, Ritchie TK, Ragueneau-Majlessi I (2020) Variability in In Vitro OATP1B1/1B3 Inhibition Data: Impact of Incubation Conditions on Variability and Subsequent Drug Interaction Predictions. Clin Transl Sci. 13: 47-52.

Panfen E, Chen W, Zhang Y, Sinz M, Marathe P, Gan J, Shen H (2019) Enhanced and Persistent Inhibition of Organic Cation Transporter 1 Activity by Preincubation of Cyclosporine A. Drug Metab Dispos. 47: 1352-1360.

Roth M, Obaidat A, Hagenbuch B (2012) OATPs, OATs and OCTs: the organic anion and cation transporters of the SLCO and SLC22A gene superfamilies. Br J Pharmacol. 165: 1260-1287.

Sane R, Cheung KWK, Kovács P, Farasyn T, Li R, Bui A, Musib L, Kis E, Plise E, Gáborik Z (2020) Calibrating the In Vitro-In Vivo Correlation for OATP-Mediated Drug-Drug Interactions with Rosuvastatin Using Static and PBPK Models. Drug Metab Dispos. 48: 1264-1270.

Sarkadi B, Price EM, Boucher RC, Germann UA, Scarborough GA (1992) Expression of the human multidrug resistance cDNA in insect cells generates a high activity drug-stimulated membrane ATPase. J Biol Chem. 267:4854-4858.

Shitara Y, Sugiyama Y (2017) Preincubation-dependent and long-lasting inhibition of organic anion transporting polypeptide (OATP) and its impact on drug-drug interactions. Pharmacol Ther. 177:67-80.

Shitara Y, Takeuchi K, Horie T (2013) Long-lasting inhibitory effects of saquinavir and ritonavir on OATP1B1-mediated uptake. J Pharm Sci. 102: 3427-3435.

Tátrai P, Schweigler P, Poller B, Domange N, de Wilde R, Hanna I, Gáborik Z, Huth F (2019) A Systematic In Vitro Investigation of the Inhibitor Preincubation Effect on Multiple Classes of Clinically Relevant Transporters. Drug Metab Dispos. 47: 768-778.

Uddin ME, Talebi Z, Chen S, Jin Y, Gibson AA, Noonan AM, Cheng X, Hu S, Sparreboom A (2021) In Vitro and In Vivo Inhibition of MATE1 by Tyrosine Kinase Inhibitors. Pharmaceutics. 13: 2004.

Vallejo M, Briz O, Serrano MA, Monte MJ, Marin JJ (2006) Potential role of trans-inhibition of the bile salt export pump by progesterone metabolites in the etiopathogenesis of intrahepatic cholestasis of pregnancy. J Hepatol. 44: 1150-1157.

Wright EM, Loo DD, Hirayama BA (2011) Biology of human sodium glucose transporters. Physiol Rev. 91: 733-794.

Yang X, Mei C, He X, He L, Lu X, Tong H, Lou Y (2022) Quantification of Venetoclax for Therapeutic Drug Monitoring in Chinese Acute Myeloid Leukemia Patients by a Validated UPLC-MS/MS Method. Molecules. 27: 1607.

Zhang L, Gorset W, Washington CB, Blaschke TF, Kroetz DL, Giacomini KM (2000) Interactions of HIV protease inhibitors with a human organic cation transporter in a mammalian expression system. Drug Metab Dispos. 28: 329-334.

Zhang Y, Zhang Y, Sun K, Meng Z, Chen L (2019) The SLC transporter in nutrient and metabolic sensing, regulation, and drug development. J Mol Cell Biol. 11: 1-13.

Footnotes

This work received no external funding.

No author has an actual or perceived conflict of interest with the contents of this article.

DMD Fast Forward. Published on May 19, 2023 as DOI: 10.1124/dmd.122.001191
This article has not been copyedited and formatted. The final version may differ from this version.

Figure Legends

Figure 1. Transporters for which $PTIP_{30min}$ ≥ 2.00 was observed, located on the SLC phylogenetic tree. Adapted from Zhang et al., 2019.

Figure 2. Correlation of highest $PTIP_{30min}$ with physicochemical parameters. Spearman's ρ and Pearson's r coefficients are shown for significant correlations. In (G), the vertical dashed line indicates the cut-off value of tPSA/MW = 0.25, which was found to be predictive of $PTIP_{30min}$ ≥ 2.00 (horizontal dashed line).

Figure 3. IC_{50} determination of inhibitors that showed apparent PTIP >20% in the vesicular transport assay. Full IC_{50} curves were taken after 30 minutes of preincubation with the inhibitor [Preinc(+)] or its solvent [Preinc(-)]. [I], concentration of the inhibitor; E3S, estrone sulfate; NMQ, N-methylquinidinium; TC, taurocholate. IC_{50} values are in μM.

Figure 4. The modifying effect of BSA, added during preincubation only, on PTIP. Charts (A) and (C) show accumulation of radiolabeled substrate (CPM, count per minute) after preincubation with the inhibitor (Preinc(+)) or its solvent (Preinc(-)) in the presence of 0%, 1%, 2%, 4%, and 5% of BSA. Charts (B) and (D) correspond to the charts in (A) and (C) and display the ratio (in percentage value) of substrate uptake in the Preinc(+) over Preinc(-) condition.

DMD Fast Forward. Published on May 19, 2023 as DOI: 10.1124/dmd.122.001191
This article has not been copyedited and formatted. The final version may differ from this version.

Figure 5. The modifying effect of BSA, added during both preincubation and coincubation, on PTIP. Charts (A) and (C) show accumulation of radiolabeled substrate (CPM, count per minute) after preincubation with the inhibitor (Preinc(+)) or its solvent (Preinc(-)) in the presence of 0%, 1%, 2%, 4%, and 5% of BSA. Charts (B) and (D) correspond to the charts in (A) and (C) and display the ratio (in percentage value) of substrate uptake in the Preinc(+) over Preinc(-) condition.

Figure 6. The effect of BSA alone on the uptake of E217βDG and metformin. Cells were preincubated with a buffer containing 0-5% w/v BSA, then incubated with the probe substrate, but no inhibitor, in the presence of the same concentration of BSA as applied during preincubation.

Figure 7. Persistence of the preincubation effect after washout with or without BSA. Preincubation with the inhibitor for 90 minutes in protein-free medium was followed by 0, 15, 30, 60, and 90 minutes of washout with medium containing 0%, 1%, or 5% w/v BSA but no inhibitor. Uptake was then measured without inhibitor or BSA.

DMD Fast Forward. Published on May 19, 2023 as DOI: 10.1124/dmd.122.001191
This article has not been copyedited and formatted. The final version may differ from this version.

Tables

Table 1. The effect of a 30-minute inhibitor preincubation on IC_{50} in SLC transporter inhibition assays. IC_{50} values are shown as mean ± SEM of N=2 measurements. IC_{50} values obtained without vs. with preincubation were compared by Student's t-test (NS: P≥0.05, *: P<0.05, **: P<0.01; ***: P<0.001). $PTIP_{30min}$ values that correspond to significant changes in IC_{50} have been highlighted in bold if between 2 and 3, and in bold and italic if greater than 3. Abbreviations: AMG, methyl-α-D-glucopyranoside; E217βG, estradiol β-D-glucuronide; CCK8, sulfated cholecystokinin octapeptide; E3S, estrone 3-sulfate, MPP+, 1-methyl-4-phenylpyridinium.

Transporter	**Probe substrate (total concentration in µM)**	**Inhibitor (concentration range in µM)**	**IC_{50}, mean of N=2 ± SEM, in µM**		**$PTIP_{30min}$**
			without preinc.	with 30-min preinc.	
ASBT, human	taurocholate (5)	taurochenodeoxycholate (0.41-300)	19.2 ± 0.5	8.37 ± 0.65**	**2.31 ± 0.24**
Asbt, rat	taurocholate (5)	taurochenodeoxycholate (1.37-1000)	48.6 ± 0.4	9.91 ± 1.32**	***4.98 ± 0.62***
ASCT1	L-serine (1)	L-cysteine (1.52-10000)	273 ± 6	146 ± 3**	1.86 ± 0.09
ASCT2	L-serine (1)	L-cysteine (1.52-10000)	793 ± 186	510 ± 176^{NS}	1.62 ± 0.20
CNT1	uridine (1)	adenosine (0.05-300)	10.7 ± 1.0	8.92 ± 1.14^{NS}	1.20 ± 0.04
CNT2	uridine (1)	adenosine (0.05-300)	3.06 ± 0.09	2.93 ± 0.33^{NS}	1.06 ± 0.15
CNT3	uridine (1)	2-deoxycytidine (0.05-300)	11.6 ± 1.1	18.8 ± 1.0*	0.62 ± 0.03
ENT1	uridine (1)	dilazep (0.003-2)	0.0403 ±	0.00420 ±	***9.61*** ±

DMD Fast Forward. Published on May 19, 2023 as DOI: 10.1124/dmd.122.001191
This article has not been copyedited and formatted. The final version may differ from this version.

			0.0018	0.00025**	***0.15***
ENT2	adenosine (1)	dipyridamole (0.014-10)	0.270 ± 0.022	0.232 ± 0.006^{NS}	1.16 ± 0.07
LAT1	L-leucine (1)	nanvuranlat (0.03-20)	0.0890 ± 0.0023	0.0139 ± 0.0004**	***6.43*** ± ***0.35***
MATE1	metformin (10)	pyrimethamine (0.001-5)	0.0897 ± 0.0098	0.0246 ± 0.0004*	***3.64*** ± ***0.33***
MATE2-K	metformin (10)	pyrimethamine (0.001-5)	0.0978 ± 0.0160	0.0282 ± 0.0020*	***3.44*** ± ***0.33***
MCT8[a]	triiodothyronine (3)	sorafenib (0.07-50)	50.0 ± 0.0	4.90 ± 0.27***	***10.2*** ± ***0.56***
MCT10	triiodothyronine (3)	imatinib (0.48-350)	191 ± 10	66.0 ± 4.6**	**2.90 ± 0.05**
NTCP, human	taurocholate (2)	taurochenodeoxycholate (0.05-300)	15.8 ± 0.6	7.87 ± 0.48**	**2.02 ± 0.20**
Ntcp, rat	taurocholate (1)	troglitazone 0.27-200)	5.37 ± 0.07	0.986 ± 0.125**	***5.55*** ± ***0.78***
OAT1	tenofovir (5)	benzbromarone (0.046-300)	5.40 ± 0.73	0.902 ± 0.049*	***6.05*** ± ***1.14***
OAT2	cGMP (1.5)	indomethacin (0.046-300)	18.8 ± 0.4	2.87 ± 0.29***	***6.65*** ± ***0.82***
OAT3	E3S (1)	probenecid (0.076-500)	6.36 ± 1.06	3.54 ± 0.40^{NS}	1.78 ± 0.10
OAT3	E3S (1)	benzbromarone (0.046-300)	0.898 ± 0.085	0.159 ± 0.009*	***5.71*** ± ***0.87***
OAT7	E3S (1)	bromosulphthalein (0.02-100)	1.23 ± 0.01	0.398 ± 0.078**	***3.20*** ± ***0.64***
OATP1B1	E217βG (1)	rifampicin (0.008-50)	1.22 ± 0.21	0.959 ± 0.113^{NS}	1.32 ± 0.38
OATP1B1	E217βG (1)	cyclosporin A (0.004-25)	0.605 ±	0.132 ±	***4.75*** ±

DMD Fast Forward. Published on May 19, 2023 as DOI: 10.1124/dmd.122.001191
This article has not been copyedited and formatted. The final version may differ from this version.

			0.091	0.018*	***1.32***
OATP1B3	CCK8 (1)	rifampicin (0.002-10)	1.61 ± 0.45	1.20 ± 0.01^{NS}	1.33 ± 0.37
OATP1B3	CCK8 (1)	cyclosporin A (0.001-5)	0.645 ± 0.042	0.292 ± 0.059*	**2.33 ± 0.62**
OATP2B1	E3S (1)	rifamycin SV (0.14-100)	3.82 ± 0.49	2.34 ± 0.04^{NS}	1.63 ± 0.24
OCT1	sumatriptan (10)	verapamil (0.046-300)	9.77 ± 2.99	5.32 ± 0.91^{NS}	1.79 ± 0.26
OCT2	metformin (10)	verapamil (0.046-300)	38.5 ± 1.0	16.4 ± 0.2**	**2.35 ± 0.09**
OCT3	MPP+ (0.02)	quinidine (1.37-1000)	308 ± 15	146 ± 33*	**2.20 ± 0.40**
RFVT3	riboflavin (0.2)	riboflavin 5-phosphate (0.15-1000)	41.3 ± 0.4	19.4 ± 1.8**	**2.15 ± 0.21**
SGLT1	AMG (1)	phloridzin (0.14-100)	0.236 ± 0.030	0.231 ± 0.014^{NS}	1.03 ± 0.19
SGLT2	AMG (1)	dapagliflozin (0.0004-0.3)	0.0283 ± 0.0032	0.0124 ± 0.0008*	**2.27 ± 0.10**
URAT1	uric acid (20)	benzbromarone (0.002-5)	0.0857 ± 0.0014	0.0265 ± 0.0033**	***3.29 ± 0.46***

[a] Without preincubation, inhibition was less than 50% at 50 µM. Therefore, the IC_{50} could not be determined but must be higher than 50 µM, and the $PTIP_{30min}$ provided here is a low-end estimate.

DMD Fast Forward. Published on May 19, 2023 as DOI: 10.1124/dmd.122.001191
This article has not been copyedited and formatted. The final version may differ from this version.

Table 2. Correlation between selected molecular features and highest observed $PTIP_{30min}$ of the inhibitors tested. Data were compiled from the ChEMBL database (https://www.ebi.ac.uk/chembl/) (molecular species classification, MW, CX LogD, CX LogP, tPSA), the ALOGPS 2.1 calculator of the Virtual Computational Chemistry Laboratory (http://www.vcclab.org/lab/alogps/) (CLogS), and DruMAP (https://adme.nibiohn.go.jp/) (PPBp, calculated as $1\text{-}f_{u,p,human}$). Some calculated descriptors, where unavailable in ChEMBL, were also taken from ALOGPS 2.1 or DruMAP, and the molecular species classification of cyclosporin A as neutral was taken from Berton et al., 2019. Highest $PTIP_{30min}$ values are the highest observed $PTIP_{30min}$ values for inhibitors that were tested on multiple transporters. N/A, not available.

Inhibitor	Mol. species	MW	CX LogD	CX LogP	tPSA	tPSA / MW	CLogS	PPB_p	Highest $PTIP_{30min}$
sorafenib	neutral	464.8	4.34	4.34	92.4	0.1988	-5.43	0.999	10.20
dilazep	base	604.7	1.14	2.88	114.5	0.1893	-4.08	0.88	9.61
indomethacin	acid	357.8	0.26	3.53	68.5	0.1915	-5.17	0.995	6.65
nanvuranlat (JPH203)	base	472.3	N/A	1.74	125.0	0.2647	-4.57	0.986	6.43
benzbromarone	acid	424.1	3.69	5.55	50.4	0.1189	-4.51	0.988	6.05
troglitazone	neutral	441.6	4.67	5.50	84.9	0.1922	-5.56	0.975	5.55
taurochenodeoxycholate	acid	499.7	-0.23	1.10	123.9	0.2480	-4.82	0.922	4.98
cyclosporin A	neutral	1202.6	4.00	3.27	278.8	0.2318	-5.10	0.997	4.75
pyrimethamine	neutral	248.7	2.23	2.75	77.8	0.3129	-3.14	0.844	3.64
bromosulphthalein	acid	794.0	2.34	7.09	175.5	0.2210	-5.00	0.992	3.20
imatinib	neutral	493.6	4.38	3.80	86.3	0.1748	-4.53	0.958	2.90
verapamil	base	454.6	2.79	5.04	64.0	0.1407	-5.06	0.916	2.35
dapagliflozin	neutral	408.9	2.11	2.11	99.4	0.2431	-3.37	0.937	2.27
quinidine	base	324.4	0.86	2.51	45.6	0.1405	-2.99	0.842	2.20
riboflavin 5-	acid	456.4	-5.67	-1.04	208.1	0.4560	-2.68	0.818	2.15

DMD Fast Forward. Published on May 19, 2023 as DOI: 10.1124/dmd.122.001191
This article has not been copyedited and formatted. The final version may differ from this version.

phosphate									
L-cysteine	zwitterion	121.2	-2.80	-2.79	63.3	0.5226	-0.72	0.553	1.86
probenecid	acid	285.4	-0.92	2.44	74.7	0.2617	-2.83	0.807	1.78
rifamycin SV	neutral	697.8	3.68	4.17	201.3	0.2885	-4.68	0.91	1.63
rifampicin	neutral	823.0	2.87	2.95	220.2	0.2675	-4.30	0.966	1.33
adenosine	neutral	267.3	-2.09	-2.09	139.5	0.5221	-1.28	0.249	1.20
dipyridamole	neutral	504.6	1.81	1.81	145.4	0.2882	-2.74	0.869	1.16
phloridzin	neutral	436.4	0.85	0.98	177.1	0.4059	-2.56	0.919	1.03
2-deoxycytidine	neutral	227.2	-1.90	-1.90	110.6	0.4868	-0.19	0.176	0.62
Correlation with highest $PTIP_{30min}$		**MW**	**CX LogD**	**CX LogP**	**tPSA**	**tPSA / MW**	**CLogS**	**PPB_p**	
Spearman's (rank), ρ		0.219	0.449	0.528	-0.296	-0.643	-0.730	0.668	
P		0.315	0.036	0.010	0.170	0.001	0.00008	0.0005	
Pearson's (parametric), r		0.161	0.362	0.412	-0.210	-0.515	-0.603	0.453	
P		0.463	0.098	0.051	0.335	0.012	0.002	0.030	

DMD Fast Forward. Published on May 19, 2023 as DOI: 10.1124/dmd.122.001191
This article has not been copyedited and formatted. The final version may differ from this version.

Table 3. IC_{50} determination of inhibitors that showed apparent PTIP >20% in the vesicular transport assay. Full IC_{50} curves were taken after 30 minutes of preincubation with the inhibitor [Preinc(+)] or its solvent [Preinc(-)]. [I], concentration of the inhibitor; E3S, estrone sulfate; NMQ, N-methylquinidinium. *, P<0.05; ^{NS}, not significant.

Transporter	Probe substrate (total concentration in µM)	Inhibitor (concentration range in µM)	IC_{50} in µM		$PTIP_{30min}$
			Preinc(-)	Preinc(+)	
BCRP	E3S (1)	eltrombopag (0.014-10)	0.336	0.253	1.33
		Ko-143 (0.001-1)	0.358	0.273	1.31
		novobiocin (0.024-100)	0.338	0.413	0.82
MDR1	NMQ (1)	pantoprazole (0.24-1000)	329	446	0.74
		sertraline (0.24-1000)	29.9	44.8	0.67
		talinolol (0.024-100)	140[a]	171[a]	0.82
		valspodar (0.004-3)	0.133	0.0598	2.22
			0.147	0.0793	1.85
		Mean	0.140	0.0696*	**2.04**
		zosuquidar (0.007-5)	0.0904	0.0421	2.15
			0.123	0.0487	2.53
		Mean	0.107	0.0454^{NS}	2.34
BSEP	TC (0.2)	rifampicin (0.274-200)	14.2	11.6	1.22

[a] Extrapolated values; talinolol at the highest concentration failed to achieve 50% inhibition.

DMD Fast Forward. Published on May 19, 2023 as DOI: 10.1124/dmd.122.001191
This article has not been copyedited and formatted. The final version may differ from this version.

Table 4. The effect of preincubation on the inhibition of BCRP and MDR1 in the monolayer assay. Data shown are mean ± SEM from N=2 experiments. Significance was calculated by Student's t-test (NS: P≥0.05).

Transporter	Probe substrate (total concentration in µM)	Inhibitor (concentration range in µM)	IC_{50} in µM		PTIP
			Preinc(-)	Preinc(+)	
BCRP	prazosin (1)	Ko-143 (0.0014-1.0)	0.0658 ± 0.0142	0.0634 ± 0.0277^{NS}	1.16 ± 0.28
		omeprazole (0.78-50)	6.74 ± 0.62	3.75 ± 0.90^{NS}	1.95 ± 0.63
		eltrombopag (0.625-40)	2.63 ± 0.57	3.05 ± 0.03^{NS}	0.86 ± 0.18
MDR1	digoxin (5)	valspodar (0.01-10)	0.412 ± 0.052	0.488 ± 0.023^{NS}	0.84 ± 0.07
		zosuquidar (0.08-5.0)	0.362 ± 0.027	0.309 ± 0.003^{NS}	1.17 ± 0.10
		quinidine (1.56-100)	9.05 ± 2.02	7.62 ± 1.59^{NS}	1.18 ± 0.02
		verapamil (1.56-100)	9.18 ± 1.01	5.98 ± 0.26^{NS}	1.54 ± 0.24

DMD Fast Forward. Published on May 19, 2023 as DOI: 10.1124/dmd.122.001191
This article has not been copyedited and formatted. The final version may differ from this version.

Table 5. The modifying effect of BSA on PTIP caused by a 30-minute preincubation. IC_{50} was measured under 6 conditions defined by the presence or absence of 5% w/v BSA during preincubation, the presence or absence of inhibitor during preincubation, and the presence or absence of inhibitor during the uptake phase of the assay. PTIP was then calculated as a ratio of IC_{50} values measured under different conditions as shown in the top row. CI, confidence interval; CsA, cyclosporin A; N/D, not determined due to incomplete or irregular IC_{50} curve.

Condition # / Calculation of PTIP	(1)	(2)	(3)	(4)	(5)	(6)	(2)/(1)	(2)/(3)	(5)/(4)	(5)/(6)
5% w/v BSA during preincubation	-	-	-	+	+	+	-	-	+	+
Inhibitor during preincubation	+	-	+	+	-	+	-/+	-/+	-/+	-/+
Inhibitor during the uptake phase	+	+	-	+	+	-	+	-	+	-
	IC_{50}, μM (95% CI)						PTIP, fold			
OATP1B1 / E217βG / venetoclax	4.97 (3.47-7.12)	166 (94.7-292)	5.22 (3.56-7.65)	18.1 (12.8-25.6)	839 (112-6250)	33.5 (21.0-53.5)	33.4	31.9	46.3	25.0
OATP1B1 / E217βG / CsA	0.0752 (0.0671-0.0842)	0.336 (0.292-0.386)	0.140 (0.120-0.163)	0.0931 (0.0765-0.113)	0.234 (0.125-0.438)	0.199 (0.165-0240)	4.5	2.4	2.5	1.2
OCT1 / sumatriptan / ledipasvir	N/D	N/D	N/D	323 (79.7-1312)	N/D	156 (51.2-477)	N/D	N/D	N/D	N/D
OCT1 / sumatriptan /	0.889 (0.713-	2.70 (1.86-	4.01 (2.73-	0.669 (0.549-	2.38 (1.60-	2.12 (1.61-	3.0	0.7	3.6	1.1

DMD Fast Forward. Published on May 19, 2023 as DOI: 10.1124/dmd.122.001191
This article has not been copyedited and formatted. The final version may differ from this version.

irinotecan	1.11)	3.91)	5.89)	0.814)	3.53)	2.80)				
OCT2 / metformin / daclatasvir	1.22 (0.911-1.64)	3.55 (2.07-6.08)	2.00 (1.45-2.77)	2.60 (1.95-3.46)	3.88 (2.39-6.30)	8.14 (5.81-11.4)	2.9	1.8	1.5	0.5
OCT2 / metformin / isavuconazole	0.400 (0.252-0.634)	1.51 (0.989-2.31)	0.455 (0.324-0.639)	1.35 (1.01-1.81)	2.38 (1.73-3.26)	1.81 (0.946-3.45)	3.8	3.3	1.8	1.3

DMD Fast Forward. Published on May 19, 2023 as DOI: 10.1124/dmd.122.001191
This article has not been copyedited and formatted. The final version may differ from this version.

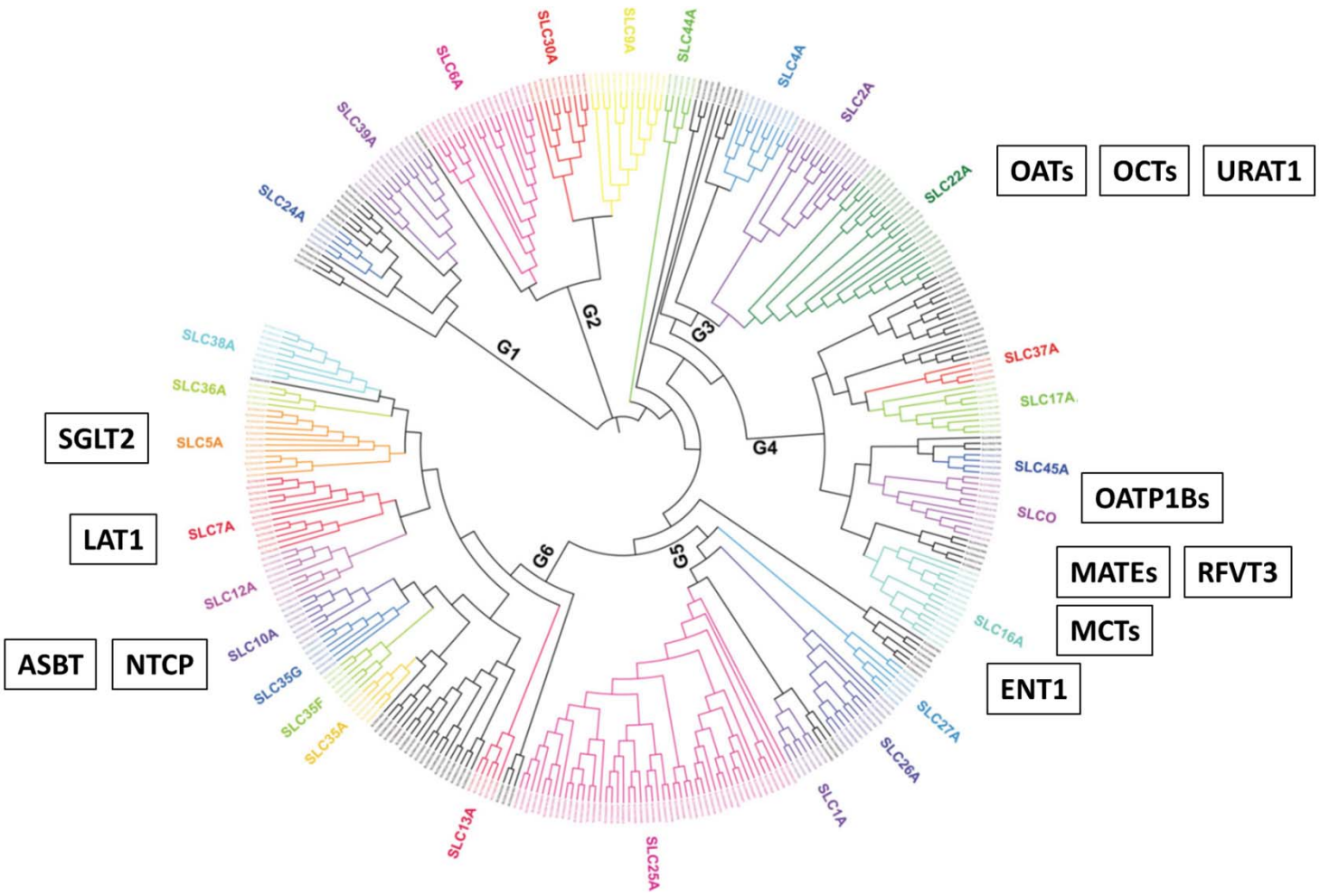

Figure 1

DMD Fast Forward. Published on May 19, 2023 as DOI: 10.1124/dmd.122.001191
This article has not been copyedited and formatted. The final version may differ from this version.

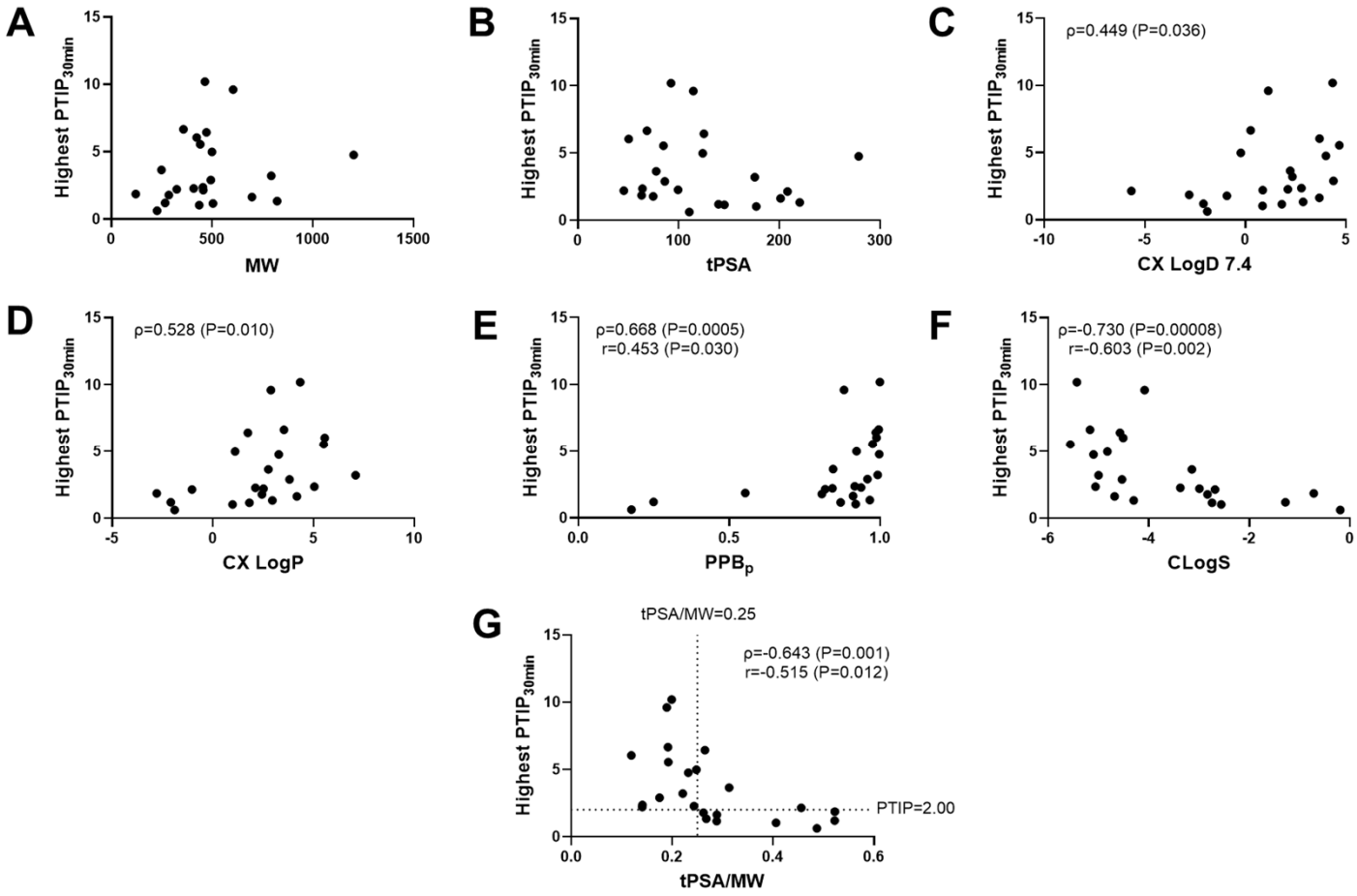

Figure 2

DMD Fast Forward. Published on May 19, 2023 as DOI: 10.1124/dmd.122.001191
This article has not been copyedited and formatted. The final version may differ from this version.

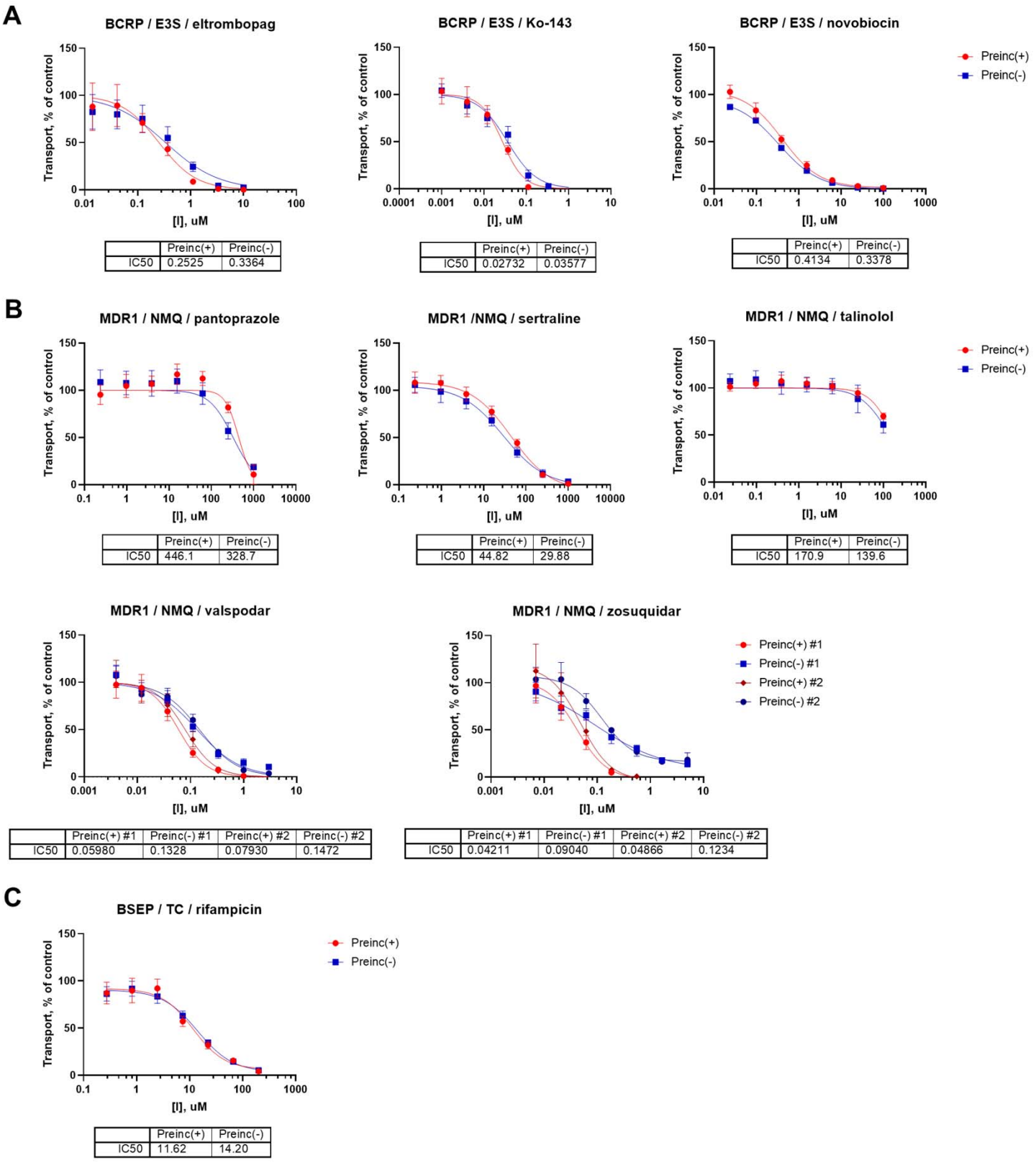

Figure 3

DMD Fast Forward. Published on May 19, 2023 as DOI: 10.1124/dmd.122.001191
This article has not been copyedited and formatted. The final version may differ from this version.

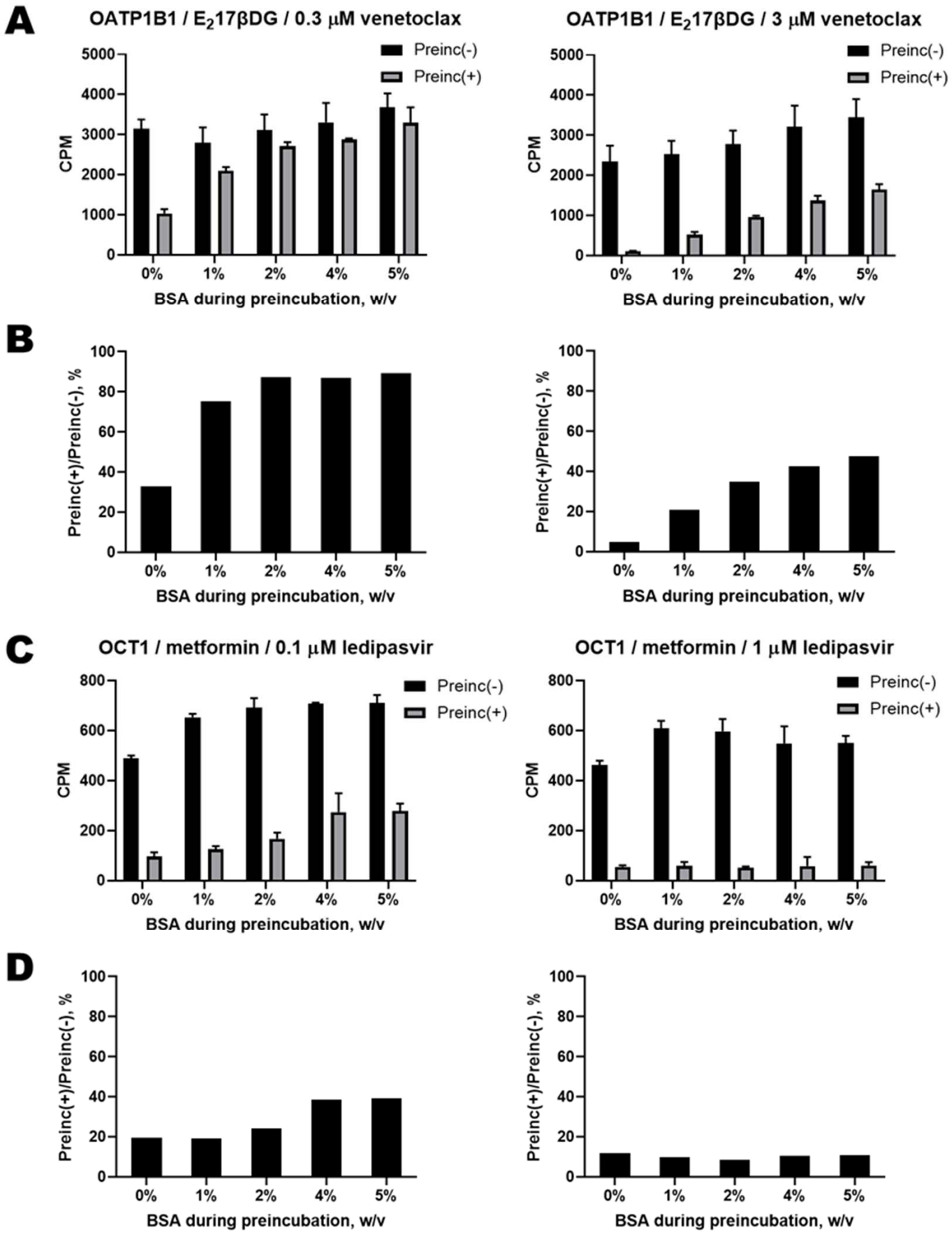

Figure 4

DMD Fast Forward. Published on May 19, 2023 as DOI: 10.1124/dmd.122.001191
This article has not been copyedited and formatted. The final version may differ from this version.

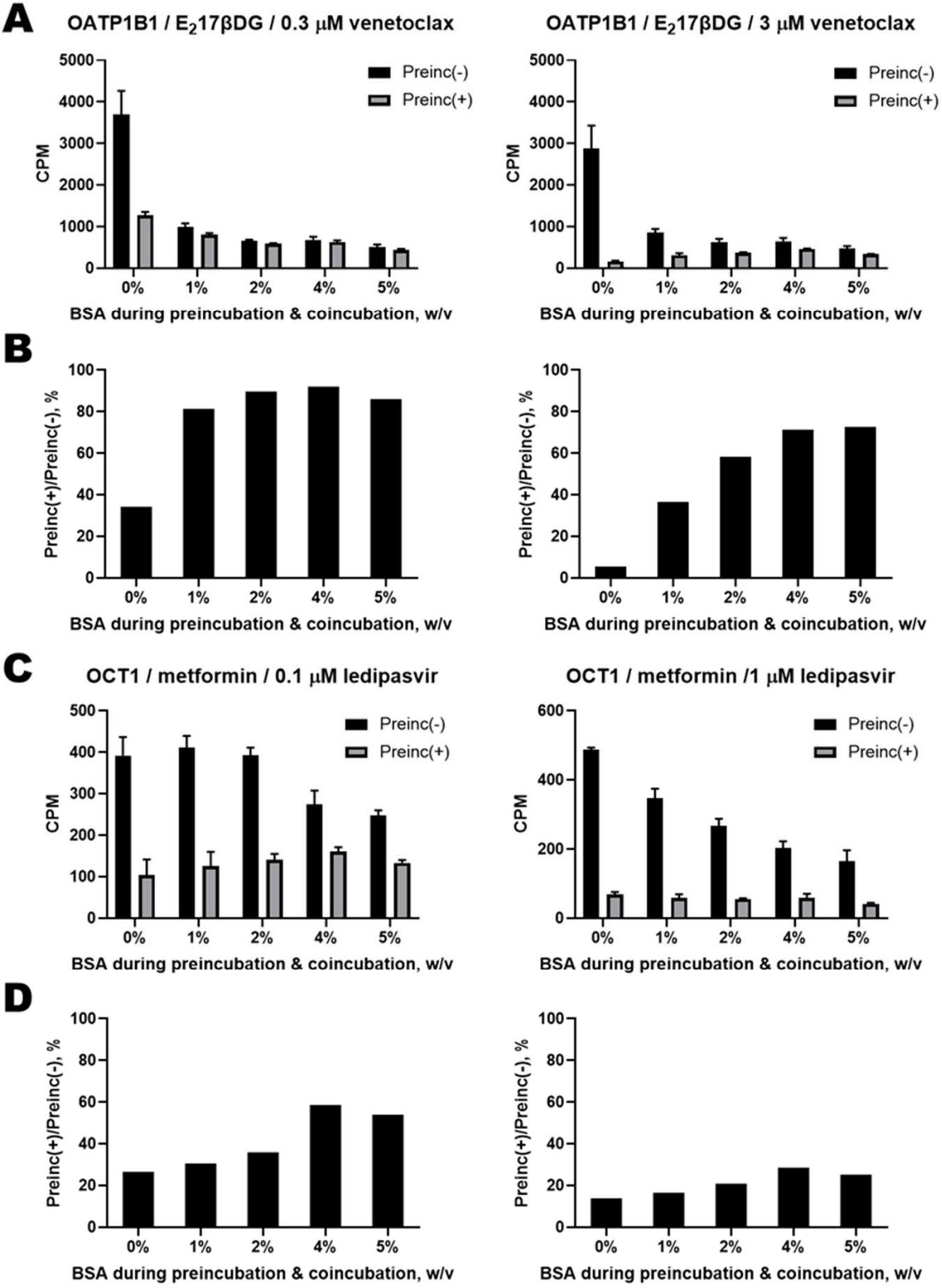

Figure 5

DMD Fast Forward. Published on May 19, 2023 as DOI: 10.1124/dmd.122.001191
This article has not been copyedited and formatted. The final version may differ from this version.

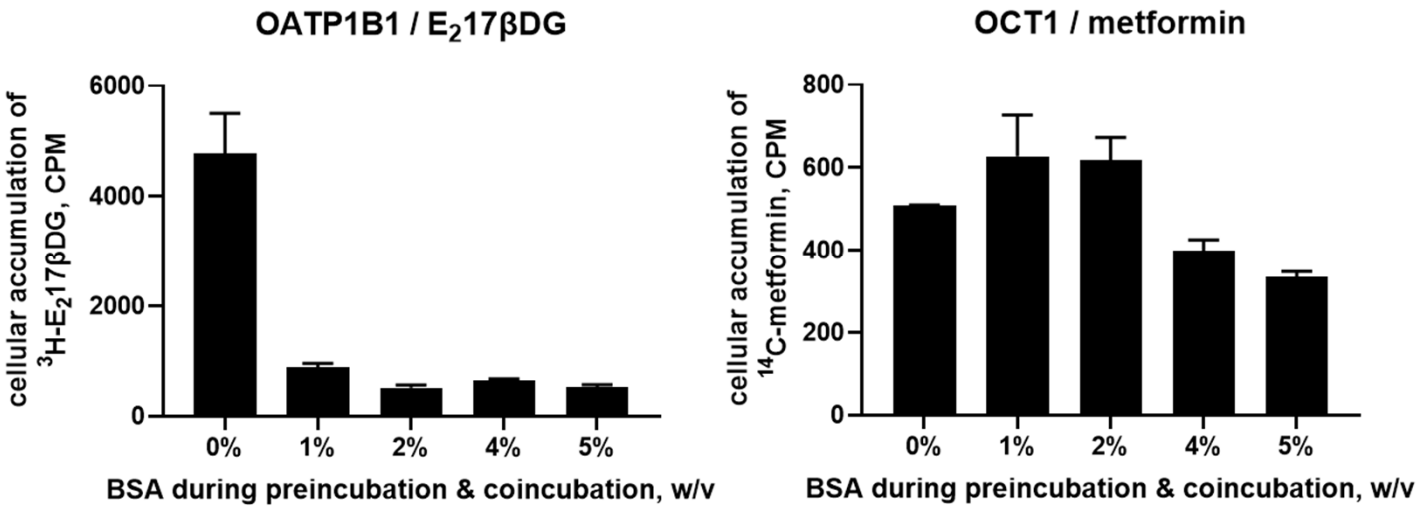

Figure 6

DMD Fast Forward. Published on May 19, 2023 as DOI: 10.1124/dmd.122.001191
This article has not been copyedited and formatted. The final version may differ from this version.

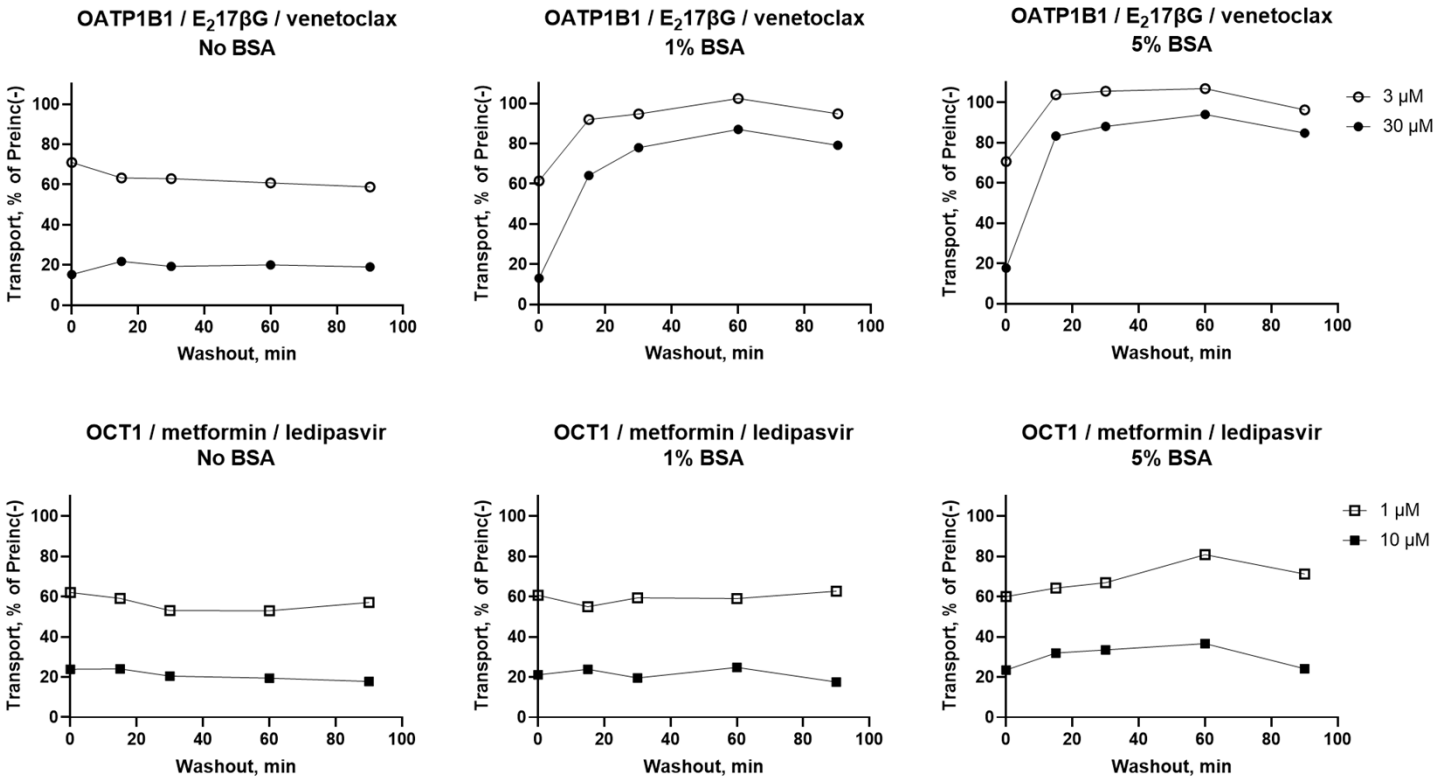

Figure 7